

Viscous attractor for the Galton board

W. G. Hoover and B. Moran

Department of Applied Science, University of California at Davis/Livermore and Lawrence Livermore National Laboratory, Livermore, California 94550

(Received 18 May 1992; accepted for publication 1 September 1992)

We analyze the Galton Board [or periodic “Lorentz Gas”] with a point mass scattered by elastic disks of diameter σ , using a constant driving field g and a constant-viscosity linear drag force $-p/\tau$, where p is the point-mass momentum. This combination leads to a nonequilibrium steady state which depends only upon the dimensionless ratio $g\tau^2/\sigma$. The long-time-averaged trajectory leads to multifractal phase-space structures closely resembling those we found earlier using isokinetic equations of motion derived from Gauss’ Principle of Least Constraint. A highly damped [small τ] creeping-flow limit describes our results for $g\tau^2/\sigma$ less than about 0.2. The lightly damped Green–Kubo linear-response limit for the model provides an accurate description of the dissipative dynamics for $g\tau^2/\sigma$ greater than about 2.0.

I. INTRODUCTION

The Galton Board (or periodic “Lorentz Gas”) is a familiar classroom and textbook antique from the early days of probability theory,¹ Brownian Motion, and statistical mechanics.² A point-mass particle, with mass m , colliding with a periodic “Board” of fixed elastic scatterers of diameter σ , and free from any other external forces, can exhibit diffusive ($\langle r^2 \rangle \propto t$) Brownian motion. Alternatively, if the motion is *driven* by a gravitational field mg and is simultaneously subject to a viscous drag force, proportional to the momentum with proportionality constant $-1/\tau$, a steady current obeying Fick’s Law and defining the conductivity $\kappa = \langle v \rangle / g$ can result. In this case, conservation of energy establishes that the time-averaged power, $\langle mgv \rangle$, provided by the field must balance the viscous power loss $\langle mv^2/\tau \rangle$, where m is the mass. For the lightly damped case $\langle v \rangle$ is much less than the thermal velocity; then the linear conductivity can be related to the kinetic temperature $T \equiv \langle mv_x^2 \rangle / k \equiv \langle mv_y^2 \rangle / k$, where v_x and v_y are the components of the thermal velocity, and k is Boltzmann’s constant.

In 1986 we investigated the phase-space distribution for a simplified “isokinetic” variant of the Board in which a colliding particle moves, in the presence of a fixed external field, with fixed kinetic energy.³ The isokinetic constraint follows Gauss’ Principle of Least Constraint.⁴ The constraint is implemented by a time-reversible constraint force $F_{\text{constraint}} \equiv -\zeta p \equiv -p/\tau$ linear in the momentum p and the friction coefficient $\zeta \equiv 1/\tau$. The resulting isokinetic “Gaussian” dynamics is a special case of isothermal “Nosé–Hoover” mechanics.⁵ This form of mechanics has by now been applied to a variety of nonequilibrium problems involving from two to more than a million atoms.⁶ It has been generalized, very recently, in several ways.⁷ We have emphasized that the motion governed by this time-reversible mechanics invariably satisfies the requirements of the Second Law of Thermodynamics.⁸ Vance has recently investigated the phase-space distribution for this same model by studying the structure of the underlying periodic orbits in phase space.⁹

The phase-space distribution underlying the isokinetic Galton-Board dynamics showed an unexpected complex structure, a “strange attractor.” This model was the first *time-reversible*, but dissipative, system to be studied and led to a comprehensive investigation of nonequilibrium steady states. In such a system the *internal* system variables, controlled by fixed *external boundary conditions*, typically fluctuate about long-term average values characterizing the “steady state.” Parallel work on a two-body shear flow was carried out by Morriss.¹⁰ The multifractal attractors generated by the Board and other more elaborate models are, we believe, typical of nonequilibrium steady-state systems. We have shown more recently that such an attractor can also result when a nonsteady transient current is induced by a nonlinear field which varies exponentially with displacement.¹¹

Because the underlying Nosé–Hoover dynamics is still a relatively new development, we are frequently asked to show that phase-space strange attractors can be generated with a “more physical” dynamics. Accordingly, we consider here another non-Hamiltonian steady-state version of the Galton-Board problem, this time with a constant-viscosity drag force proportional to velocity. Thus the drag force has the same functional form as has “Stokes’ drag,” which describes the retardation of three-dimensional creeping flow in a viscous medium. Although the generalization from two space dimensions to three is straightforward we believe that nothing is gained by the additional complexity and restrict ourselves here to the two-dimensional case. Even so, the two-dimensional motion takes place in a four-dimensional phase space (x, y, p_x, p_y) with a three-dimensional subspace $(\alpha, \sin \beta, |p|)$ required to detail the sequence of collisions which makes up the motion. See Fig. 1 for the definitions of α and β . We will demonstrate here that the three-dimensional space required to display the collisions contains a multifractal attractor similar to those which appear in the two-dimensional space $(\alpha, \sin \beta)$ describing the isokinetic Galton Board.³

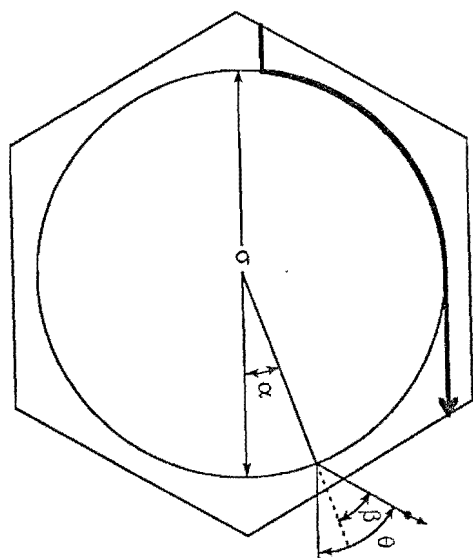


FIG. 1. Our computational cell, used to follow the motion, is half of the unit crystallographic cell shown here. The angles α and β which characterize the scattering collisions are indicated. The "creeping-flow" trajectory which results in the limiting conductivity $\kappa/\tau=0.514$ is shown as a heavy line with an arrow.

II. MODEL (Refs. 2 and 3)

For simplicity we choose again a triangular (sixfold coordinated) lattice of elastic scatterers, (hard disks of diameter σ). We choose a density equal to $4/5$ the maximum close-packed density, so that scattering is inevitable. Under these conditions a mass point falls (in the negative y direction) under the influence of a gravitational field g and with a retarding force $-p/\tau$. The motion can be studied in half of a single unit cell of the lattice by using periodic boundary conditions. As is shown in Fig. 1, the field direction is chosen perpendicular to one of the three sets of parallel close-packed atomic rows which make up the triangular lattice structure.

The equations of motion are

$$m d^2 x / dt^2 = dp_x / dt = -p_x / \tau,$$

$$m d^2 y / dt^2 = dp_y / dt = -mg - p_y / \tau.$$

The motion is independent of the mass m . The motion equations can be integrated (with respect to time) to give the time development of the momentum between collisions:

$$p_x = p_x(0) e^{-t/\tau}, \quad p_y + mg\tau = [p_y(0) + mg\tau] e^{-t/\tau}.$$

Another integration gives the coordinate-space trajectory of the motion:

$$x = x(0) + p_x(0) (\tau/m) [1 - e^{-t/\tau}],$$

$$y = y(0) - gt\tau + [p_y(0) (\tau/m) + g\tau^2] [1 - e^{-t/\tau}].$$

At each elastic scatterer collision the sign of the radial momentum of the moving particle is reversed. For convenience, and without loss of generality, we choose the mass m , and the viscous relaxation time τ equal to unity.

TABLE I. Reduced conductivity κ/τ as a function of the dimensionless ratio $g\tau^2/\sigma$, for a particle colliding with a periodic triangular-lattice array of scatterers at a density 80% of the closest-packed density. The scatterer diameter is σ . The mean time between collisions is Δt . As $g\tau^2/\sigma$ approaches 0 (strong damping) the moving particle collides repeatedly with a single scatterer, "rolling" along its perimeter, as shown in Fig. 1. In the opposite (lightly damped) limit, as $g\tau^2/\sigma$ approaches ∞ , the speed approaches ∞ while the distance between collisions, of order σ , is fixed. Thus again the mean time between collisions approaches 0.

$g\tau^2/\sigma$	κ/τ	$\Delta t/\tau$
0.05	0.482	0.003 57
0.08	0.464	0.042 7
0.10	0.445	0.131
0.15	0.406	0.341
0.20	0.365	0.476
0.30	0.280	0.498
0.40	0.159	0.095 8
0.50	0.277	0.817
0.60	0.319	1.10
0.80	0.267	0.953
1.00	0.203	0.667
1.25	0.198	0.613
1.50	0.197	0.524
1.75	0.192	0.443
2.00	0.182	0.379
3.00	0.138	0.278
5.00	0.0959	0.198
10.00	0.0591	0.127
20.00	0.0370	0.082 2
50.00	0.0199	0.045 4
100.00	0.0125	0.028 9
200.00	0.0080	0.018 2
400.00	0.0051	0.011 5
500.00	0.0044	0.009 8

By introducing *reduced* (dimensionless) coordinates $\{x/\sigma, y/\sigma\}$, and a reduced time t/τ , it is easy to show that the *shape* of the trajectory depends only on the dimensionless ratio $g\tau^2/\sigma$. Likewise the reduced (dimensionless) conductivity $\kappa/\tau \equiv \langle v \rangle / g\tau$ depends solely on $g\tau^2/\sigma$. From the thermodynamic standpoint $g\tau^2/\sigma$ is the ratio of the steady-speed kinetic energy $K_{\text{drift}} \approx m(g\tau)^2$ to the potential energy change required to cross a periodic cell of the Board, $\Delta\Phi \approx mg\sigma$. From the standpoint of fluid mechanics $g\tau^2/\sigma$ is the Reynolds number of the flow, the product of a characteristic length $L = \sigma$ and a characteristic velocity $v = g\tau$, divided by the kinematic viscosity, $\nu \equiv \sigma^2/\tau$.

$$\begin{aligned} K/\Delta\Phi &\approx m(g\tau)^2/mg\sigma \equiv g\tau^2/\sigma \equiv \sigma(g\tau)/(\sigma^2/\tau) \\ &\approx \text{Re} \equiv Lv/\nu \approx \sigma(g\tau)/(\sigma^2/\tau). \end{aligned}$$

III. SIMULATION OF THE MOTION

Following the lines established in our previous work³ we have generated here a series of a million collisions at several representative values of the dimensionless ratio $g\tau^2/\sigma$. Results for the conductivity are shown in Table I and Fig. 2. Because the ratio of the thermal velocity to the drag velocity is of order τ/κ , the lightly damped limit [with long decay time τ] corresponds to large values of the dimensionless combination $g\tau^2/\sigma$. In the lightly damped case

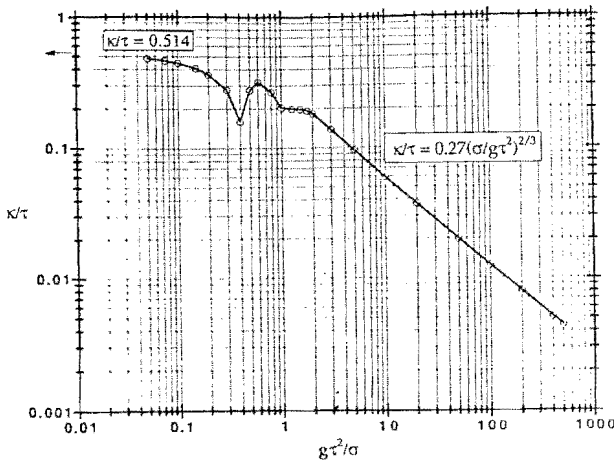


FIG. 2. Reduced conductivity, κ/τ , as a function of dimensionless ratio $g\tau^2/\sigma$. The data were obtained from a series of runs involving one million elastic scatterer collisions each. The arrow to the left indicates the strongly damped “creeping-flow” theoretical estimate. The solid line to the right indicates the lightly damped Green-Kubo theoretical estimate, $\kappa/\tau=0.27(\sigma/g\tau^2)^{2/3}$.

we found, as expected, a conductivity agreeing with that found previously at this same scatterer density,

$$\kappa \equiv \langle v \rangle / g \approx 0.1\sigma(m/kT)^{1/2}.$$

This lightly damped value is also consistent with Machta and Zwanzig’s equilibrium Green-Kubo estimate² and is further discussed in the following section.

For values of the ratio $g\tau^2/\sigma$ on the order of unity, phase-space plots of successive collisions indicate that the motion is chaotic. In the extreme case, where the “thermal velocity” (meaning: fluctuation of the velocity about the mean value, as a function of vertical coordinate) is negligibly small, the trajectories converge to the limit cycles illustrated in Fig. 1. To illustrate a typical chaotic case (for a field of moderate strength, $g\tau^2/\sigma=10$) we show the last 20 000 collisions as a stereo pair. See Fig. 3. The abscissa gives the location of each collision relative to the field direction, an angle α lying between 0 and π . The ordinate gives the sine of the angle β describing the direction of motion just after collision relative to the radial vector from the scatterer to the moving particle. The remaining direc-

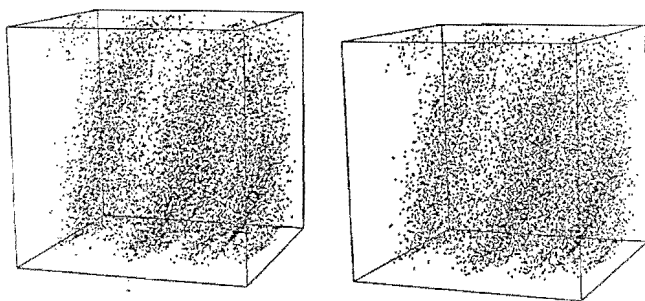


FIG. 3. Stereo view of 20 000 successive collisions $\{\alpha, \sin \beta, p\}$ of a particle colliding with a periodic triangular-lattice array of scatterers at a density equal 80% of the closest-packed arrangement. The dimensionless ratio $g\tau^2/\sigma$ is 10.

tion in the plot indicates the speed at which the collision characterized by α and β took place. The same data could alternatively be displayed in only two dimensions by using color to identify the particle speed. It is readily apparent that the strange attractor is a multifractal. The multifractal spectrum could be estimated using standard techniques, though we have not chosen to do this.

IV. ANALYSIS OF LIMITING CASES

Two different limiting cases can be analyzed. When the effect of the field is only a minor perturbation on the thermal motion the conductivity can be calculated from Green-Kubo linear-response theory. This conductivity corresponds to our earlier weak-field measurement³ as well as to Zwanzig and Machta’s Green-Kubo result.² In this limit we found

$$\kappa \equiv v_{\text{DRAG}}/g = 0.10\sigma(m/kT)^{1/2}, \quad 2kT \equiv m[\langle v_x^2 \rangle + \langle v_y^2 \rangle].$$

Notice that the conductivity has units of time. The reduced conductivity κ/τ is dimensionless. In this same limit, where the thermal velocity greatly exceeds v_{DRAG} , we can relate the temperature to the field by using conservation of energy. The time-averaged power loss due to friction, $\langle p^2/m\tau \rangle$ must match the time-averaged power provided by the field, $mgv_{\text{DRAG}} = mg^2\kappa$:

$$\langle p^2/m\tau \rangle \equiv 2kT/\tau \equiv mgv_{\text{DRAG}} = mg^2\kappa.$$

Solving for the thermal velocity, $(kT/m)^{1/2}$, gives

$$(kT/m)^{1/2} = 0.707(\kappa\tau)^{1/2}g.$$

It should be emphasized that in this limit the thermal velocity greatly exceeds the field-induced velocity v_{DRAG} .

Combining this last equation with the Green-Kubo result $\kappa \equiv 0.10\sigma(m/kT)^{1/2}$ leads to a useful expression for the reduced conductivity:

$$\kappa/\tau = 0.27(\sigma/g\tau^2)^{2/3}.$$

In Fig. 2 the extensive sampling of numerical results for the reduced conductivity, κ/τ , as a function of the ratio $g\tau^2/\sigma$ for values greater than about 2 shows a slope of $-2/3$, just as predicted by this Green-Kubo analysis.

On the other hand for [strongly damped] ratios less than $g\tau^2/\sigma=0.2$, an alternative dynamical estimate for the creeping-flow conductivity describes the data. In this regime, between collisions the moving particle falls at the “terminal velocity”, $g\tau$, for the total “free-fall” distance $x_1+x_2=0.47174\sigma$ indicated in Fig. 1. The “collisions” which alternate with these free-fall trajectory segments involve rolling (with a speed proportional to the cosine of the angle between the direction of motion and the field direction). Taking the total distance traveled divided by the total time leads to the creeping-flow estimate:

$$\kappa/\tau = 0.514,$$

indicated by the arrow at the left margin of Fig. 3. This estimate agrees very nicely with the “low-field” data.

V. TIME REVERSIBILITY AND NONEQUILIBRIUM STEADY STATES

Time reversibility arises in a natural way in nonequilibrium steady states. In Gaussian isokinetic mechanics the friction coefficient ζ is proportional to the time rate-of-change of the potential energy. In Nosé's original derivation of Nosé-Hoover isothermal dynamics the friction coefficient ζ starts out as a momentum.⁵ Thus in both kinds of mechanics ζ changes sign in the reversed motion and *the trajectories can be followed either forward or backward in time using the same motion equations*. An equivalent pictorial definition of time reversibility is this: if a movie of a time-reversible motion is projected backwards (with the order of the frames reversed) the resulting "reversed" motion still satisfies *the same* motion equations. Motions obeying the Second Law of Thermodynamics invariably convert work to heat, not the other way around. Nevertheless any Gaussian or Nosé-Hoover trajectory could (*in principle*) be reversed to generate a trajectory *violating* the Second Law by converting heat to work. The apparent paradox of nonequilibrium steady states (invariably obeying the *irreversible* Second Law of Thermodynamics with *time-reversible* equations of motion) has been traced to the multifractal nature of the underlying phase-space attractor. Although phase-space states which can violate the Second Law of Thermodynamics do exist, they are invariably restricted to a multifractal mechanically unstable phase-space repeller which has zero volume relative to the equilibrium phase space.⁸ There is thus no way to follow such states in time.

Despite the straightforward nature of the time-reversibility concept several workers have (incorrectly) claimed that the Nosé-Hoover equations of motion are not time reversible.¹² In the present case the friction coefficient $\zeta = 1/\tau$ is intrinsically positive and the dynamics is therefore dissipative. Nevertheless *in principle even this irreversible trajectory could be followed backward in time*, apart from computer roundoff errors, simply by changing the sign of the friction coefficient, setting the relaxation time τ equal to $-\tau$. *In practice*, a Lyapunov-unstable time-reversed trajectory can be followed accurately for only a few collisions. The exponential growth of the inevitable roundoff errors guarantees that any longterm numerical solution with positive friction will diverge rather than return to the initial condition.

VI. CONCLUSION

The multifractal attractors generated here using a relatively conventional linear-drag-force approach show a qualitative resemblance to those generated with Gaussian or Nosé-Hoover mechanics. For weak to moderate field strengths the motion describing this nonequilibrium steady state is confined to a multifractal strange attractor. For weakly damped motion the resulting conductivity agrees with the Green-Kubo dependence established earlier. For strong damping the conductivity agrees with a simple creeping-flow calculation.

ACKNOWLEDGMENTS

Joanne L. Levatin (Earth Sciences Division, LLNL) very kindly provided the software which generated the stereo Fig. 3. In addition to our traditional thanks to the National Science Foundation for generous travel support we would like to thank Brad Holian (LANL) and Aurel Bulgac (Michigan State University) for the discussions that led to this extension of our 1987 work. The referees' comments were particularly helpful. This work was performed, in part, at the Lawrence Livermore National Laboratory under the auspices of the Department of Energy under the provisions of Contract No. W-7405-Eng-48.

¹M. Kac, *Scientific American* **211**(9), 92 (1964).

²J. Machta and R. W. Zwanzig, *Phys. Rev. Lett.* **50**, 1959 (1983).

³B. Moran, W. G. Hoover, and S. Bestiale, *J. Stat. Phys.* **48**, 709 (1987).

⁴W. G. Hoover, *Computational Statistical Mechanics* (Elsevier, Amsterdam, 1991), pp. 21-23.

⁵S. Nosé, *J. Chem. Phys.* **81**, 511 (1984); *Mol. Phys.* **52**, 255 (1984); *Prog. Theor. Phys. Suppl.* **103**, 1 (1991); W. G. Hoover, *Phys. Rev. A* **31**, 1695 (1985).

⁶W. G. Hoover, A. J. DeGroot, and C. G. Hoover, *Comput. Phys.* **6**, 155 (1992).

⁷D. Kusnezov, A. Bulgac, and W. Bauer, *Ann. Phys.* **204**, 155 (1990); **214**, 180 (1992); R. G. Winkler, *Phys. Rev. A* **45**, 2250 (1992); G. J. Martyna, M. L. Klein, and M. Tuckerman, *J. Chem. Phys.* **97**, 2635 (1992).

⁸W. G. Hoover, H. A. Posch, B. L. Holian, M. J. Gillan, M. Mareschal, and C. Massobrio, *Mol. Simulations* **1**, 79 (1987); B. L. Holian, W. G. Hoover, and H. A. Posch, *Phys. Rev. Lett.* **50**, 10 (1987).

⁹W. N. Vance, *Phys. Rev. Lett.* **69**, 1356 (1992).

¹⁰G. P. Morriss, *Phys. Lett. A* **122**, 236 (1987).

¹¹W. G. Hoover, B. Moran, C. G. Hoover, and W. J. Evans, *Phys. Lett. A* **133**, 114 (1988).

¹²See, for instance, D. C. Wallace, "Computer Simulation of Nonequilibrium Processes," in *Shock Waves in Condensed Matter*, edited by Y. M. Gupta (Plenum, New York, 1986), p. 42; P. Gaspard and F. Baras, "Dynamical Chaos Underlying Diffusion in the Lorentz Gas," in *Microscopic Simulations of Complex Hydrodynamic Phenomena*, edited by M. Mareschal and B. L. Holian (Plenum, New York, 1992), p. 301.